

Holocene variations in the Asian monsoon inferred from the geochemistry of lake sediments in central Tibet

Carrie Morrill ^{a,*}, Jonathan T. Overpeck ^{a,b}, Julia E. Cole ^a, Kam-biu Liu ^c,
Caiming Shen ^c, Lingyu Tang ^d

^a *Geosciences Department, Gould-Simpson Building, University of Arizona, Tucson, AZ 85721, USA*

^b *Institute for the Study of Planet Earth, 715 N. Park Avenue (2nd Floor), University of Arizona, Tucson, AZ 85721, USA*

^c *Department of Geography and Anthropology, Louisiana State University, Baton Rouge, LA 70803, USA*

^d *Nanjing Institute of Geology and Palaeontology, Chinese Academy of Sciences, Nanjing 210008, China*

Received 20 June 2004

Available online 2 February 2006

Abstract

We present a record of monsoon variations for the early and middle Holocene that is inferred from the geochemistry of sediment cores from Ahung Co, a lake in central Tibet. The resolution of this record is better than 50 yr and the age model is derived from radiocarbon ages of terrestrial charcoal, which eliminates errors associated with the lake hard-water effect. We made down-core geochemical measurements of % carbonate, % organic carbon, C/N and $\delta^{13}\text{C}$ of bulk organic matter, $\delta^{13}\text{C}$ and $\delta^{18}\text{O}$ of carbonate, and % dolomite. Proxy calibration and modern water-balance reconstruction show that these are proxies for lake depth and the amount of monsoon precipitation. We find that lake level and monsoon precipitation have been decreasing at Ahung Co since the early Holocene (~7500 cal yr B.P.). Superimposed on this trend are rapid declines in monsoon rainfall at 7000–7500 and 4700 cal yr B.P. and seven century-scale wet–dry oscillations. The cores do not contain sediment from the last ~4000 yr. Surface sediments from the lake accumulated during the 20th century, however. From this, we argue that lake levels have risen again recently following a late Holocene dry period.

© 2005 University of Washington. All rights reserved.

Keywords: Precipitation; Monsoon; Holocene; Climate change; Oxygen stable isotopes; Paleoclimate; Hard-water effect; Aquatic macrophytes

Introduction

The Asian summer monsoon is one of the most important components of Earth's climate system. Monsoon extremes cause flooding and droughts that impact nearly half of the world's population. In addition, the Asian monsoon may affect climate globally, through interactions with El Niño (e.g., Shukla and Paolino, 1983; Liu et al., 2000) and mid-latitude circulation (e.g., Wang et al., 2001).

It is well established that the Asian monsoon weakened through the Holocene in response to the gradual decrease in summer insolation (e.g., Prell and Kutzbach, 1992; Overpeck et al., 1996; An et al., 2000). Recently, higher-resolution records

have provided hints of abrupt climate transitions and fluctuations superimposed upon this gradual trend (e.g., Gasse and Van Campo, 1994; Guo et al., 2000; Morrill et al., 2003; Overpeck et al., 2005). Resolution, age control and spatial coverage are, however, currently insufficient to develop a detailed picture of regional monsoon variability on decadal to century timescales.

In this research, we develop a century-scale record of monsoon variations during the early and middle Holocene based on the water-balance history of Ahung Co (Co = lake) in Tibet. Tibet is an excellent place to study the Asian monsoon for three reasons. First, the present-day limit of monsoon rainfall crosses Tibet, causing this region to be particularly sensitive to monsoon variations (Fig. 1). Second, the Tibetan Plateau plays an important role in initiating and maintaining the monsoon circulation. During the summer, a strong latitudinal temperature gradient exists in the upper troposphere due in part to heating of the atmosphere over the

* Corresponding author. Current address: Climate and Global Dynamics Division, National Center for Atmospheric Research, 1850 Table Mesa Drive, Boulder, CO 80305, USA. Fax: +1 303 497 1348.

E-mail address: morrill@ucar.edu (C. Morrill).

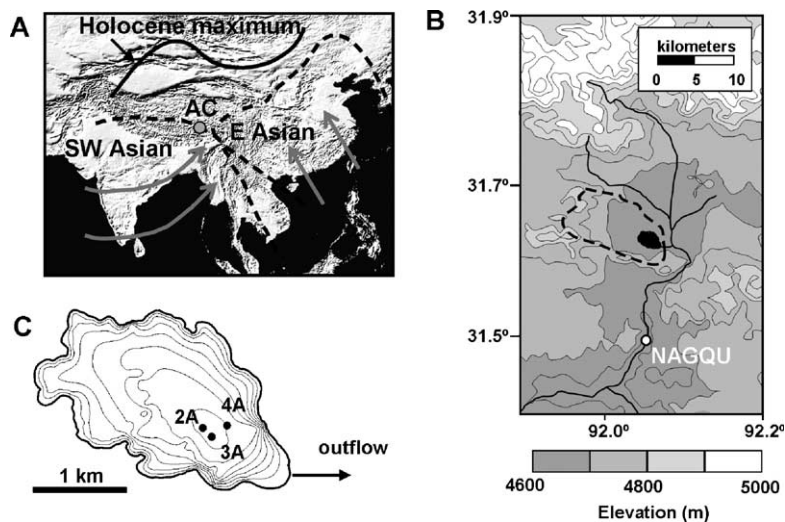


Figure 1. (A) Estimated present extent of southwest Asian and east Asian monsoons (Araguas-Araguas et al., 1998) and maximum extent of monsoons during Holocene (Winkler and Wang, 1993). (B) Ahung Co and surrounding area, contour interval is 100 m, dashed line indicates extent of surface drainage basin and solid lines show rivers and streams. (C) Ahung Co bathymetry measured in July 2001, contour interval is 20 cm and circles show core locations.

plateau. This gradient fuels the monsoon circulation. Surface and climatic conditions on the plateau, which impact tropospheric heating, can play an important role in modulating the monsoon circulation (e.g., Barnett et al., 1988). Third, the environment of Tibet has been relatively undisturbed by human activities. Intensive agriculture and settlement in other parts of the monsoon region, including India and eastern China, add a complicating factor to proxy records (e.g., Hodell et al., 1999).

Despite the motivation for developing monsoon records from Tibet, few records exist from this region and those that do have uncertain age models. The age models of two Tibetan ice cores that span the Holocene were estimated by extrapolation of annual layer thickness and correlation to the GISP2 ice core (Thompson et al., 1989, 1997). Due to a lack of terrestrial macrofossils, age models for Tibetan lake records have been based on radiocarbon dates of aquatic material. These lakes have hard-water effects as large as 3200 yr (Fontes et al., 1996), however, and possible variations in the hard-water effect through time were not taken into account in every case (Gasse et al., 1991, 1996; Lister et al., 1991; Morinaga et al., 1993). This new record from Ahung Co has an accurate age model based on more than 50 radiocarbon dates of both aquatic material and terrestrial charcoal.

Study area

Ahung Co is a small (3.6 km²) freshwater lake located in the steppe of central Tibet (31.62°N, 92.06°E). This region has relatively low topographic relief; the elevation of the lake is 4575 m and elevations in its drainage basin are up to 4900 m (Fig. 1). The area of the lake's surface drainage basin is about 100 km². There are several streams that discharge water into the wetlands surrounding the lake, but none of these streams flow directly into the lake. Ahung Co has a small surface outlet and the lake level currently oscillates above and below the level

of this outlet. Mean lake depth in July 2001 was about 1 m and maximum lake depth was about 1.5 m.

The region surrounding Ahung Co is underlain by Mesozoic sedimentary and metasedimentary rocks (Chang et al., 1988). Outcrops in the basin consist of quartzite, shale and small amounts of dolomite. Vegetation in the basin consists of marsh meadows composed of Cyperaceae and steppe dominated by *Artemisia* and *Stipa* (Shen, 2003).

The mean annual air temperature in this area is about -1.5°C , and patches of permafrost are present in some locations (Wang and French, 1995). Average air temperature during January is about -13°C and during July is about 9°C . Annual precipitation is between 30 and 60 cm, with about 80% falling from June to September during the summer monsoon.

A detailed water-balance study of Ahung Co and its drainage basin over the past 16 yr showed that present-day water-balance fluctuations are caused primarily by variations in the amount of summer monsoon precipitation (Morrill, 2004). Decreased lake and basin evaporation during humid monsoon summers further amplifies the response of lake level to monsoon variations.

Methods

Core collection

We collected three sediment cores from Ahung Co during July 1995 and July 1999 using a modified Livingstone piston corer (Wright et al., 1984) and a floating platform. These cores, designated 2A, 3A and 4A, were collected from the deepest part of the lake, which was under about 1.5 m of water in July 2001 (Fig. 1). All three cores are 1 m long or less; an unidentified, unpenetrable layer exists below this depth. The main visual feature of each of these cores is a nearly identical pattern of alternations between layers dominated by the aquatic macrophyte *Potamogeton* and layers consisting primarily of lacustrine carbonate (Fig. 2).

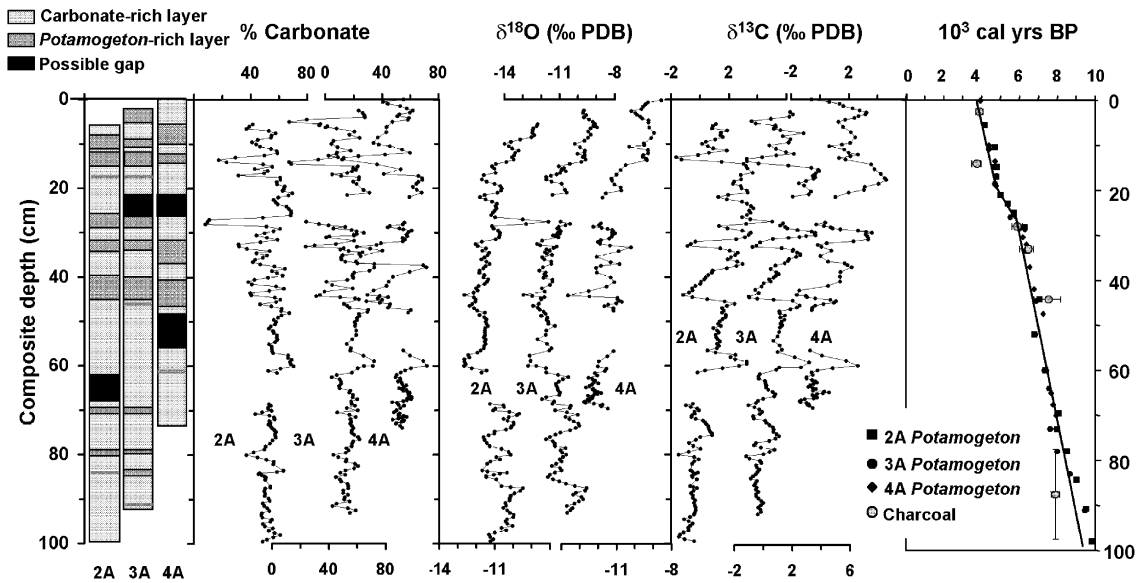


Figure 2. Correlation of Ahung Co cores 2A, 3A and 4A and age model used for cores. The composite depth scale on the y axis is a scale to which each core was correlated. Gaps in the time-series indicate periods of erosion and/or non-deposition determined by curve matching of proxy time-series.

Radiocarbon dating

The bedrock in the basin of Ahung Co contains some carbonate rocks, including dolomite and shales with calcareous cement. Thus, we expect that radiocarbon ages of aquatic material are older than their actual time of deposition due to the lake hard-water effect (e.g., Deevey et al., 1954). This is confirmed from radiocarbon dates on living, submerged aquatic plants (*Potamogeton* spp.) collected from the lake in July 2001. In alkaline waters (pH > 8) where aqueous CO₂ is limited, these plants use bicarbonate for photosynthesis (Lucas et al., 1978) and their ages reflect the hard-water effect. Three samples of *Potamogeton* yield an average ¹⁴C activity of 99.8% (Table 1). Given a ¹⁴C activity of atmospheric CO₂ in 2001 of ~108% (S. Trumbore, unpublished data), the present hard-water correction for *Potamogeton* in Ahung Co is 600 to 700 yr.

To generate an age model that does not reflect the hard-water effect, we used terrestrial charcoal from core sediment. Charcoal was identified under a microscope and picked using tweezers. Due to the small amounts of charcoal in these cores, it was necessary to combine samples from corresponding intervals in multiple cores. We correlated the cores to the 1-cm level using

measurements of % carbonate, δ¹⁸O and δ¹³C of bulk carbonate, and *Potamogeton* radiocarbon ages (Fig. 2); these correlations also agree with those based on fine-scale visual stratigraphy of *Potamogeton* layers. Charcoal is scarce in the lower half of the cores and we obtained only one radiocarbon measurement from these depths (Table 2). This date (UCIT 3388) was measured using charcoal and terrestrial fly fragments from a 20-cm length of sediment near the bottom of core 2A.

Due to the very small size of these charcoal samples (e.g., 100 to 200 μg of carbon), we measured the δ¹³C value of only one sample. This value (−24.1‰) is distinct from the δ¹³C value of *Potamogeton*, the primary aquatic plant (~−10‰), but is close to values obtained for modern steppe plants surrounding the lake (~−25 to −27‰). We conclude that steppe plants are the likely source of this charcoal.

We calculated calendar ages of all radiocarbon dates using the CALIB radiocarbon calibration program v. 4.3 and the calibration dataset of Stuiver et al. (1998). Four of the six charcoal dates are not statistically different from the ages of *Potamogeton* from the same depth. The remaining two charcoal samples, AA44634 and UCIT3388, are younger than *Potamogeton* samples from the same depth (Table 2, Fig. 2).

Table 1
Radiocarbon measurements of living *Potamogeton* and surface sediments

Lab #	Water depth of sample (cm)	mg of carbon	δ ¹³ C (‰ PDB)	¹⁴ C activity (% of modern)	Apparent age*
<i>Potamogeton</i> growing in lake July 2001					
AA44630	120	1.12	−10.9	99.19 ± 0.47	680 ± 40
AA44630	120	0.87	−10.5	99.99 ± 0.46	620 ± 40
AA44630	120	0.84	−14.1	100.13 ± 0.46	610 ± 40
<i>Bulk organic matter in surface sediments</i>					
AA46141	45	1.04	−23.1	96.48 ± 0.37	
AA46142	47	1.05	−23.1	98.83 ± 0.63	
AA46142	47	2.50	−23.1	92.86 ± 0.60	

* Apparent age calculated using a modern ¹⁴C activity of 108% (2001 conditions).

Table 2
Radiocarbon dates from sediment cores

Lab #	Core	Composite depth (cm)	mg of carbon	$\delta^{13}\text{C}$ (‰ PDB)*	^{14}C age	Calendar age (median with 2 σ error range)
<i>Charcoal samples</i>						
AA50259	3A	2–4	0.10	N/A	3600 \pm 70	4090 (3890) 3690
AA44634	2A, 3A	8–10, 11–13	0.19	N/A	3480 \pm 90	3980 (3790) 3480
AA44636	2A, 3A	22–24, 20.5–22	0.20	–24.1	5090 \pm 80	6160 (5890) 5610
AA44638	2A, 3A	27–29, 27–29	0.15	N/A	5710 \pm 200	6990 (6490) 6000
AA44640	2A, 3A	38–40, 39–41	0.16	N/A	6640 \pm 340	8160 (7540) 6760
UCIT3388 ^a	2A	67–87	~0.20	N/A	7070 \pm 90	8110 (7900) 7680
<i>Potamogeton samples</i>						
AA41587	2A	0–1	1.26	–11.2	3810 \pm 60	4410 (4180) 3990
AA41589	2A	5–6	1.08	–10.6	4160 \pm 50	4830 (4700) 4530
AA42472	2A	9.5–10	0.87	–7.3	4250 \pm 40	4860 (4830) 4650
AA46143	2A	12–12.5	0.78	–6.5	4200 \pm 50	4850 (4820) 4550
AA46144	2A	16–16.5	0.50	–5.0	4430 \pm 50	5290 (5010) 4860
AA47723	2A	18–18.5	0.96	–5.4	4640 \pm 40	5470 (5420) 5300
AA46145	2A	20–20.5	0.87	–8.8	4990 \pm 60	5990 (5720) 5600
AA41591	2A	23–23.5	0.94	–11.6	5510 \pm 50	6410 (6290) 6200
AA42473	2A	28–29	1.22	–12.6	5660 \pm 50	6620 (6420) 6310
AA42474	2A	39–39.5	1.13	–13.0	6180 \pm 50	7250 (7090) 6910
AA47724	2A	47–47.5	0.97	–11.6	5980 \pm 60	6980 (6780) 6670
AA46146	2A	55–55.5	0.65	–10.9	6430 \pm 70	7460 (7370) 7250
AA47725	2A	58.5–58	0.80	–12.7	7240 \pm 60	8180 (8060) 7880
AA47241	2A	63–63.5	0.75	–11.3	7210 \pm 60	8170 (7990) 7880
AA47726	2A	68–68.5	1.11	–13.7	7740 \pm 60	8630 (8500) 8400
AA46147	2A	73–73.5	0.93	–11.0	8050 \pm 50	9080 (9010) 8770
AA47727	2A	80–80.5	0.78	–12.8	8570 \pm 60	9680 (9540) 9470
AA46148	2A	87–87.5	1.08	–18.1	8800 \pm 60	10,150 (9850) 9560
AA41588	3A	0–1	1.15	–9.1	3610 \pm 50	4080 (3900) 3730
AA41590	3A	8–9	0.99	–11.3	3940 \pm 30	4500 (4410) 4290
AA42475	3A	12.5–13	1.01	–11.3	4110 \pm 40	4820 (4610) 4450
AA47729	3A	15.5–16	1.17	–6.7	4200 \pm 40	4840 (4820) 4570
AA47730	3A	17.5–18	1.06	–7.8	4170 \pm 50	4840 (4720) 4530
AA47240	3A	19.5–20.5	1.19	–10.2	4780 \pm 50	5600 (5510) 5330
AA41592	3A	21.5–22	0.94	–10.9	5260 \pm 40	6170 (5990) 5920
AA42476	3A	28–29	1.01	–10.8	5600 \pm 50	6490 (6370) 6290
AA42477	3A	40.5–41	0.76	–10.8	6070 \pm 80	7210 (6900) 6690
AA47728	3A	48–48.5	1.10	–12.2	6060 \pm 40	6970 (6820) 6800
AA47242	3A	52.5–53.5	1.36	–10.4	6400 \pm 60	7430 (7320) 7210
AA47731	3A	57–57.5	0.78	–11.9	6700 \pm 50	7660 (7570) 7480
AA47732	3A	62–62.5	0.86	–11.0	7200 \pm 40	8150 (7990) 7880
AA47243	3A	65.5–66.5	0.69	–11.5	6740 \pm 50	7680 (7600) 7510
AA47733	3A	71–71.5	0.93	–13.9	7210 \pm 50	8160 (7990) 7880
AA47734	3A	76–76.5	0.86	–12.2	7900 \pm 60	9000 (8670) 8540
AA47735	3A	84–84.5	0.64	–13.7	8420 \pm 70	9540 (9460) 9160
AA41585	4A	0–1	0.94	–12.2	3640 \pm 50	4090 (3940) 3780
AA42466	4A	8.5–9	1.04	–11.4	3920 \pm 40	4500 (4410) 4240
AA42467	4A	12–12.5	1.12	–10.2	4170 \pm 50	4840 (4720) 4530
AA47719	4A	16–16.5	0.95	–6.9	4190 \pm 50	4850 (4750) 4530
AA47720	4A	20–20.5	0.88	–11.8	5500 \pm 40	6400 (6290) 6200
AA47991	4A	23–23.5	1.33	–10.8	5390 \pm 40	6290 (6200) 6000
AA42468	4A	25–25.5	1.09	–11.5	5610 \pm 50	6490 (6360) 6290
AA42469	4A	28.5–29	1.22	–12.3	5760 \pm 50	6720 (6550) 6410
AA42470	4A	32–32.5	1.21	–11.6	5950 \pm 50	6590 (6770) 6660
AA42471	4A	38.5–39	1.10	–11.3	6310 \pm 50	7410 (7250) 7030
AA47244	4A	40.5–41	1.02	–9.6	6530 \pm 70	7570 (7430) 7280
AA47245	4A	47–47.5	1.00	–12.5	6890 \pm 100	7940 (7680) 7570
AA47721	4A	54–54.5	0.86	–15.6	6960 \pm 40	7920 (7770) 7670
AA47722	4A	58–58.5	0.84	–12.6	7130 \pm 40	8100 (7940) 7860
AA47246	4A	65–65.5	0.98	–11.4	6840 \pm 60	7790 (7670) 7580

^a Sample also contained terrestrial fly fragments.

* Samples marked N/A have no $\delta^{13}\text{C}$ measurements.

The age of sample AA44634 is assumed to be inaccurate because it does not agree with other charcoal dates and would require an age reversal in the sediments. Sample UCIT3388 spans a 20-cm interval, but most of the material is derived from the upper several centimeters of this interval. The age of UCIT3388 and the age of *Potamogeton* from this smaller interval are not significantly different.

From this, we conclude that the hard-water effect was small (<600–700 yr) and relatively constant through time. We base the age model for these cores on the four consistent charcoal dates and the *Potamogeton* dates, which are fit best by three lines with inflection points at 20 cm and 28 cm (Fig. 2). This fit implies a period of lower sedimentation rate between 5000 and 6000 cal yr B.P. *Potamogeton* dates also indicate that sedimentation rates were lower in cores 3A and 4A than in core 2A during this interval. Fine-scale correlation of geochemical time-series from these cores suggest that cores 3A and 4A lack a 6-cm length of sediment present in core 2A (Fig. 2). The significance of this will be discussed in later sections. Similar gaps also seem to occur from 48 to 56.5 cm in core 4A and from 61.5 to 68.5 cm in core 2A (Fig. 2). We chose not to add inflection points to the age model at these intervals because the gaps occur in only one core and radiocarbon dates from the other cores do not show a change in sedimentation rate.

Geochemical measurements

We measured % carbonate and the $\delta^{18}\text{O}$ and $\delta^{13}\text{C}$ of bulk carbonate for all three cores for the purpose of core correlation. For core 3A, we measured additional variables for a more complete record of past variations in monsoon strength. This section describes our measurement methods and the next section discusses how the sediment geochemistry reflects past environmental and climatic change.

We measured the percent by weight of total carbon (TC) and inorganic carbon (IC) in bulk sediment at 0.5-cm intervals using a UIC Coulometrics model 5011 coulometer in the University of Arizona (UA) Geosciences Department. Reagent-grade CaCO_3 standards indicate measurement errors less than 0.02% by weight. Percent total organic carbon (TOC) was calculated as the difference between TC and IC. We calculated the percent of carbonate (CaCO_3) by multiplying IC by 8.3, which is a scaling factor that accounts for the atomic mass of calcium and oxygen.

We measured the $\delta^{18}\text{O}$ and $\delta^{13}\text{C}$ of bulk carbonate and of carbonate encrustations that precipitated inorganically around the stems of *Potamogeton*. Measurements were made in the UA Geosciences Department using a Micromass Optima mass spectrometer with automated common acid bath carbonate preparation device. Analytical precision, based on replicate measurements of a carbonate standard, was $\pm 0.02\text{‰}$ $\delta^{13}\text{C}$ and $\pm 0.07\text{‰}$ $\delta^{18}\text{O}$. In addition, we measured the $\delta^{18}\text{O}$ of surface water and precipitation samples from 1995 and 2001 on, respectively, a VG SIRA mass spectrometer with CO_2 equilibration automated preparation device at the Institute for Arctic and Alpine Research at the University of Colorado and a Finnigan Delta S mass spectrometer with CO_2 equilibration

automated preparation device at UA. The analytical precision is $\pm 0.05\text{‰}$ $\delta\delta^{18}\text{O}$.

The carbon-to-nitrogen ratio (C/N) and $\delta^{13}\text{C}$ were measured for several modern plant samples and also for bulk organic matter in core sediments at 1-cm intervals. To remove inorganic carbon from core sediments, we treated all samples with 8% sulfurous acid using the technique of Verardo et al. (1990). This method has several advantages over other techniques for carbonate-rich sediments: (1) excess acid is released as SO_2 gas, which eliminates the need for multiple rinsing steps during which sample can be lost, (2) samples are completely decalcified, and (3) water is not retained by hygroscopic salts (Verardo et al., 1990). Samples were analyzed on a Finnigan Delta Plus with Elemental Analyzer interface at UA. The standard deviations of replicate analyses of an acetanilide standard were ± 0.12 C/N and $\pm 0.04\text{‰}$ $\delta^{13}\text{C}$.

We measured the percent by volume of dolomite in the non-organic fraction of bulk sediment using X-ray diffraction methods. We removed organic matter from samples by treatment with 5% NaOCl (commercial Clorox) for 3 days. Previous studies indicate that this treatment causes no dissolution of carbonate minerals and is also the most effective for removing organic material (Gaffey and Bronnimann, 1993). Our analysis of several samples before and after this treatment verifies that the treatment did not alter any mineral diffraction patterns.

We generated diffractograms for 50 mg of each sample using a Siemens D-500 X-ray diffractometer with $\text{CuK}\alpha$ radiation at UA. We calculated the area of dolomite's major peak by multiplying the peak height and the peak width at half-height. This calculation approximates the actual peak area well and eliminates problems associated with overlapping peaks (Moore, 1989). To calibrate the relationship between XRD peak area and mineral percent, we analyzed artificial mixtures with known amounts of dolomite. By comparing known and measured values, we estimate that our calculated values are accurate to within $\pm 1\%$.

Proxy interpretations

Carbonate and organic carbon

The percents of carbonate and organic carbon are negatively correlated and reflect alternations between *Potamogeton*-rich layers and carbonate-rich layers (Fig. 3). The carbonate in this core consists primarily of calcitic micrite and aragonitic encrustations that formed on the stems of the aquatic macrophyte *Potamogeton*, but also contains small quantities of gastropods, ostracods, and detrital grains. *Potamogeton* fragments in the core are several centimeters long and were deposited horizontally in densely-packed layers. In the lake today, *Potamogeton* grows in water depths between 40 and 110 cm (Fig. 4). Water depth has a strong effect on the distribution of aquatic macrophytes, affecting macrophytes by decreased light availability in deep water and by mechanical damage by ice and exposure in shallow water (Blindow et al., 1993). The carbonate-rich intervals lacking *Potamogeton* more likely formed in waters >110 cm, not <40 cm. If the lake were only

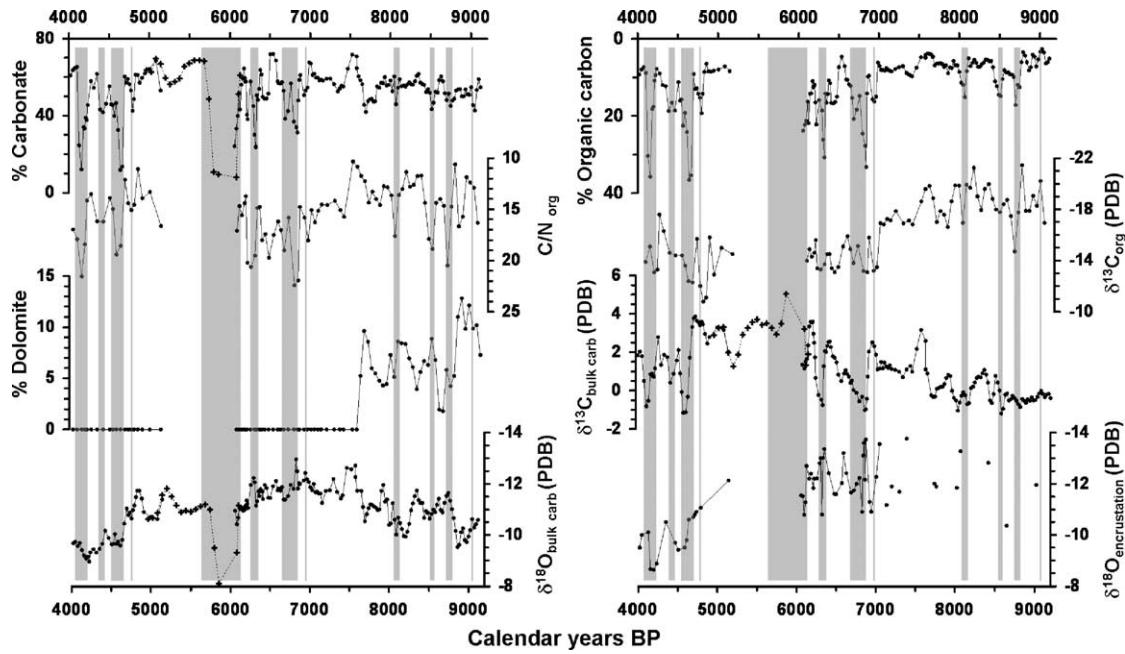


Figure 3. Proxies measured from Ahung Co core 3A. All y axes are oriented such that periods of higher lake level and/or increased monsoon precipitation plot towards the top of the figure. Gap indicates period of erosion and/or non-deposition. Shading shows intervals of abundant *Potamogeton*. Crosses and dashed lines show measurements from core 2A that span the gap in core 3A.

40 cm deep, it would be closed. The presence of *Planorbiiid* gastropods that require freshwater (Baker, 1945) and $\delta^{18}\text{O}$ values indicative of overflowing conditions (see below) argue against this possibility.

C/N and $\delta^{13}\text{C}$ organic

Variations in the C/N ratio and $\delta^{13}\text{C}$ of bulk organic matter reflect changes in the relative amounts of lacustrine algae, which are the dominant organic material in carbonate-rich intervals, and *Potamogeton*. Intervals of low (high) C/N and low (high) $\delta^{13}\text{C}$ are dominated by algae (*Potamogeton*) (Fig. 5). Terrestrial plant material, with the exception of small quantities of charcoal, is not present in the sediments. While the C/N ratio shows fine-scale variations corresponding to individual *Potamogeton*-rich intervals, $\delta^{13}\text{C}$ values only record the major increase in *Potamogeton* around 7000 cal yr B.P. (Fig. 3). This might be explained by the competing influence of large changes in the $\delta^{13}\text{C}$ of lake dissolved inorganic carbon (DIC) during these short-scale fluctuations (see below).

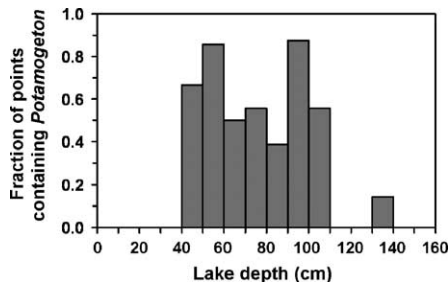


Figure 4. Occurrence of *Potamogeton* with depth in Ahung Co derived from observations during July 2001 of the presence or absence of *Potamogeton* at 110 points distributed throughout the lake.

Dolomite

There are several possible sources for dolomite in lake sediments. These include: (1) direct precipitation from saline lake water, (2) precipitation as a cement during diagenesis of lake sediments, (3) loess deposition, and (4) detrital dolomite transported by water from bedrock sources in the drainage basin. The last possibility is the simplest explanation for the presence of dolomite, since near-shore surface sediments contain pebbles of detrital dolomite. It is unlikely that loess is the source because loess in Tibet typically consists mostly of quartz and clay minerals (50–90%), with small (0–3%) amounts of dolomite (Pewe et al., 1995).

$\delta^{13}\text{C}$ carbonate

Fluctuations in $\delta^{13}\text{C}$ values of bulk carbonate correspond with the amount of *Potamogeton* preserved in the sediment

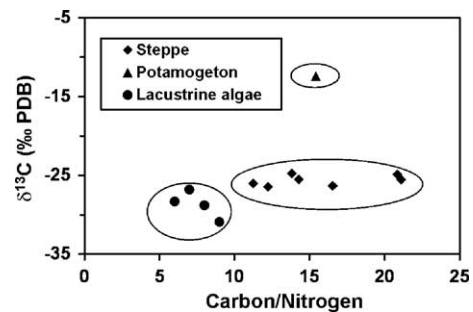


Figure 5. C/N and $\delta^{13}\text{C}$ values for three categories of organic matter. Steppe plants and *Potamogeton* were collected at Ahung Co during July 2001. Measurements for lacustrine algae were collected from Asian and North American lakes (Meyers, 1994).

(Fig. 3). This might be explained by the fact that *Potamogeton* discriminates less against ^{13}C during photosynthesis than do lacustrine algae, causing lake DIC to have a more negative $\delta^{13}\text{C}$ value when photosynthesis is dominated by *Potamogeton*. The isotopic compositions of *Potamogeton* and lacustrine algae are different enough (about 10‰) to make this a potentially large effect.

$\delta^{18}\text{O}$ carbonate

Variations in the $\delta^{18}\text{O}$ of bulk carbonate may reflect changes in one or more of the following factors: (1) lake temperature at the time of carbonate precipitation, (2) the relative amounts of aragonite and calcite, (3) the relative amount of detrital carbonate, (4) the $\delta^{18}\text{O}$ values of lake water. It is unlikely that changes in $\delta^{18}\text{O}$ values were caused primarily by changes in lake temperature because lake temperature must change 4.5°C to yield a 1‰ change in $\delta^{18}\text{O}$ value (Grossman and Ku, 1986). Similarly, variations in the amount of aragonite, which is enriched in ^{18}O relative to calcite formed under the same conditions by about 0.6 to 0.9‰ (e.g., Grossman and Ku, 1986), are too small to explain the $\delta^{18}\text{O}$ variations (not shown).

Detrital dolomite is present in the bottom third of the core. Fluctuations in the amount of dolomite are strongly positively correlated to variations in $\delta^{18}\text{O}$ (Fig. 6). The relationship between % dolomite and carbonate $\delta^{13}\text{C}$ is not as strong (not shown). This is probably because the $\delta^{13}\text{C}$ values of the dolomite, a marine carbonate ($\sim 0\text{‰}$ PDB), are similar to the $\delta^{13}\text{C}$ values of the lake carbonate (-2 to 4‰ PDB).

Using the relationship between the % dolomite and $\delta^{18}\text{O}$ (Fig. 6), we estimate that the $\delta^{18}\text{O}$ value of the dolomite is 4.8‰ PDB. Ideally, this value would be obtained from dolomite collected from the basin. One dolomite sample we collected from near-shore surface sediments yields a $\delta^{18}\text{O}$

value of -5.4‰ PDB. The difference in these values might be explained by our inability to completely remove lacustrine carbonate precipitates from the dolomite sample. In the absence of a trustworthy value from a dolomite sample, we used our estimated value (4.8‰) and a mass balance calculation to correct for the presence of dolomite. The resulting curve agrees better with most of the $\delta^{18}\text{O}$ measurements made from *Potamogeton* encrustations, which we measured whenever possible to eliminate the contribution of detrital calcite (Fig. 6). The $\delta^{18}\text{O}$ values of these two materials are similar, although values from bulk carbonate are less variable because they reflect conditions averaged over ~ 50 yr as opposed to several months.

In the upper two thirds of the core, detrital dolomite is absent and the trend of the $\delta^{18}\text{O}$ of bulk carbonate agrees with the $\delta^{18}\text{O}$ of authigenic encrustations (Fig. 6). This trend must be caused by changes in the $\delta^{18}\text{O}$ of lake water, which is a function of (1) the $\delta^{18}\text{O}$ of precipitation and (2) the residence time of water in the lake and/or catchment. Today, both factors are dependent on the amount of monsoon precipitation (Morrill, 2004). First, summer monsoon precipitation, which is derived from the Indian and/or Pacific oceans and falls from large frontal systems, is generally between -15 and -20‰ , as opposed to precipitation from local convective systems, which is derived from continental water sources and has values typically between -5 and -10‰ . This is shown by our limited measurements in 2001 (Table 3) as well as more extensive sampling by Tian et al. (2001) at Nagqu. The low $\delta^{18}\text{O}$ values of monsoon precipitation are due to progressive rain-out of the monsoon air masses as they move inland (Araguas-Araguas et al., 1998). Second, as discussed previously, Morrill (2004) showed that recent water-balance fluctuations in Ahung Co are caused primarily by variations in monsoon precipitation.

The effects of monsoon precipitation on the $\delta^{18}\text{O}$ of lake water are especially clear today. In July 1995, after several years of below-average monsoon precipitation, the lake was closed and the $\delta^{18}\text{O}$ of lake water was $+2.3\text{‰}$ (Table 3). By July 2001, several years of above-average monsoon rainfall raised the lake level to overflowing and $\delta^{18}\text{O}$ fell to -9.5‰ SMOW (Table 3).

Assuming summer water temperatures between 10° and 20°C , conditions observed in July 2001, we calculate that sediment carbonates must have precipitated from water between -9 and -14‰ SMOW. Based on this and the $\delta^{18}\text{O}$ of lake water in 1995 and 2001, we conclude that the lake was not closed for any extended period of time during the period of sediment deposition.

Inferred lake-level and monsoon history

We used principal component analysis (PCA) to identify the major transitions and fluctuations that are common to our expanded suite of proxies from core 3A. For the PCA we used the time-series shown in Figure 3, with three exceptions. First, we excluded % organic carbon because it is strongly anticorrelated with % carbonate ($r^2 = 0.58$) due

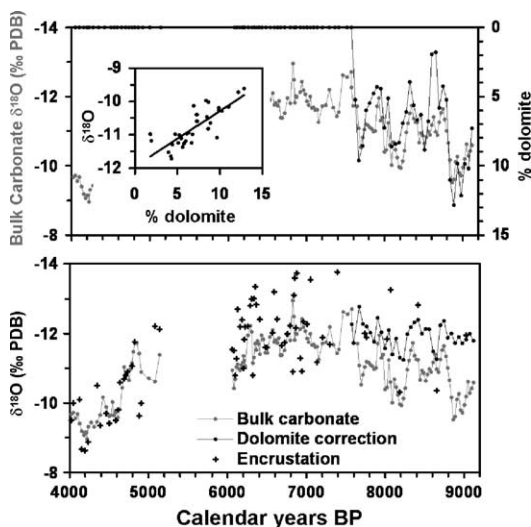


Figure 6. Correction of bulk carbonate $\delta^{18}\text{O}$ measurements in core 3A for the presence of dolomite. Top: Time-series of bulk carbonate $\delta^{18}\text{O}$ (gray) and % dolomite (black) and their correlation. Bottom: Measured $\delta^{18}\text{O}$ of bulk carbonate (gray), corrected $\delta^{18}\text{O}$ of bulk carbonate (black dots) and measured $\delta^{18}\text{O}$ of *Potamogeton* encrustations (black crosses).

Table 3
 $\delta^{18}\text{O}$ values of lake water and rainfall

Sample	Collection date	$\delta^{18}\text{O}$ (‰ VSMOW)
<i>Ahung Co lake water</i>		
Center of lake	23 July 1995	2.27
Center of lake	23 July 1995	2.27
Center of lake	23 July 1995	2.31
Shore of lake	9 July 2001	−9.85
Outflow	12 July 2001	−9.62
Shore of lake	12 July 2001	−9.10
Center of lake	12 July 2001	−9.30
<i>Precipitation</i>		
Convective storm, Nagqu	8 July 2001	−2.91
Frontal storm, Ahung Co	10 July 2001	−18.86
Frontal storm, Nagqu	10 July 2001	−16.38
Frontal storm, Nagqu	11 July 2001	−17.20

to dilution. Excluding % carbonate instead, or excluding any of the other time-series, does not change the results (not shown). Second, we used the $\delta^{18}\text{O}$ time-series corrected for the presence of dolomite (Fig. 6). Last, we excluded the low-resolution time-series of $\delta^{18}\text{O}$ values measured from encrustations.

Using the graphical test described by Wilks (1995), we determined that the first three principal components contain important information. The first PC shows a trend with greatest change between 7000 and 7500 cal yr B.P. (Fig. 7). The second PC shows multi-century oscillations that correspond to alternations between *Potamogeton*-rich and carbonate-rich layers. Phases of these oscillations that align with *Potamogeton*-rich intervals are labeled A–G in Figure 7. The third PC shows a step change at ~4700 cal yr B.P. Climatic interpretation of these events is as follows:

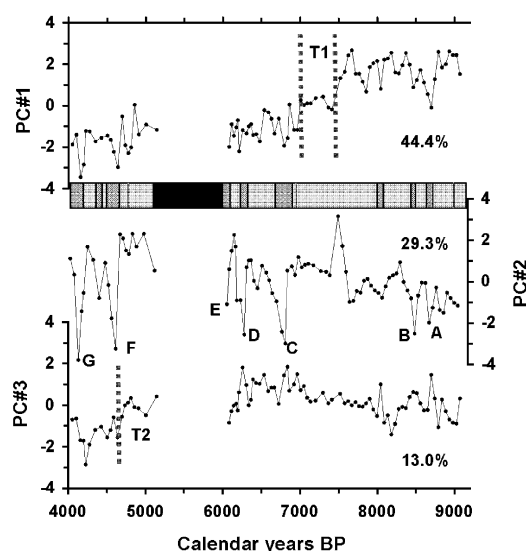


Figure 7. First three principal components calculated for six proxies from core 3A. All y axes are oriented such that periods of higher lake level and/or increased monsoon precipitation plot towards the top of the figure. Percent of total variance in the time-series explained by the principal component shown on right. Lithologic column shows intervals of abundant *Potamogeton*, as in Figure 2. T1 and T2 indicate periods of rapid change. Letters A–G identify times of peak dryness during multi-century oscillations.

Transition 1 (7000–7500 cal yr B.P.)

The first PC is significantly correlated with five of the six proxies used in the PCA (Table 4). Two of these proxies, C/N and $\delta^{13}\text{C}_{\text{organic}}$, indicate that the amount of *Potamogeton* increased sharply between 7000 and 7500 cal yr B.P. This agrees with the % carbonate and % organic carbon time-series, which show the first significant growth of *Potamogeton* at the core site at this time (Fig. 3). The increase in *Potamogeton* was likely due to a decrease in lake level to depths more suitable for its growth. We emphasize, however, that *Potamogeton* growth responds non-linearly to lake depth (Fig. 4). Thus, a gradual decrease in lake level could produce an abrupt increase in *Potamogeton* abundance.

Of the other proxies, detrital dolomite decreased abruptly to below the detection limits (1–2%) of our XRD analysis around 7500 cal yr B.P. This might indicate a reduction in runoff from the drainage basin. In addition, $\delta^{18}\text{O}$ values declined following this transition, reflecting increased residence time and/or less monsoon precipitation. The correlation between the first PC and the $\delta^{13}\text{C}$ of bulk carbonate is more difficult to interpret because of possible effects of dolomite deposition on $\delta^{13}\text{C}$ values before 7500 cal yr B.P. Overall, we argue that the first PC reflects a decrease in lake level and monsoon precipitation through the Holocene, with the greatest change occurring between 7000 and 7500 cal yr B.P. following an early Holocene monsoon maximum.

Multi-century oscillations

Alternations between *Potamogeton*-rich intervals and intervals dominated by carbonate and algal remains are clearly shown by the second PC (Fig. 7), though they are muted before 7000 cal yr B.P. when the lake was perhaps too deep at the core site for significant *Potamogeton* growth. Similar alternations occur in shallow lakes in many regions of the world (e.g., Blindow et al., 1993; Engel and Nichols, 1994; Coops and Doef, 1996). These states might represent two stable equilibria in shallow lakes (e.g., Scheffer et al., 1993). In one state, lacustrine algae dominate. They form blooms in the surface water and reduce the transparency of lake water, which prevents macrophyte growth. In the other state, transparency is increased and aquatic macrophytes, such as *Potamogeton*, dominate. Macrophytes suppress algal growth by harboring zooplankton that graze phytoplankton and by releasing sub-

Table 4
 Correlation coefficients of proxy time-series and principal components

Proxy	PC #1	PC #2	PC #3
% Carbonate	0.35	0.79	0.24
C/N ratio	−0.64	−0.58	0.40
$\delta^{13}\text{C}_{\text{organic}}$	−0.93	0.00	0.20
% Dolomite	0.80	−0.36	0.14
$\delta^{13}\text{C}_{\text{carbonate}}$	−0.45	0.81	0.00
$\delta^{18}\text{O}_{\text{carbonate}}$	−0.65	0.00	−0.71

Correlation coefficients statistically significant at the 99.9% confidence level are in bold.

stances toxic to the algae (Scheffer et al., 1993). Macrophytes also improve water clarity by reducing resuspension of bottom material. Environmental disturbances cause the system to shift between the two states. These disturbances include changes in lake level, sediment or nutrient loading, ice thickness, or wind mixing (Blindow et al., 1993; Coops and Doef, 1996; Engel and Nichols, 1994).

In the case of Ahung Co, we argue for two reasons that *Potamogeton*-rich intervals formed when the monsoon was weaker and water levels were lower. First, *Potamogeton* growth in Ahung Co is clearly dependent on water depth (Fig. 4). Second, we find some correspondence between *Potamogeton*-rich intervals and periods of more enriched $\delta^{18}\text{O}$ measured from encrustations (Fig. 3). This extends to core 2A, as well, where enriched $\delta^{18}\text{O}$ values between 5800 and 6100 cal yr B.P. correspond with an interval of particularly abundant *Potamogeton* (Fig. 3).

Low $\delta^{18}\text{O}$ values measured from the core indicate that Ahung Co overflowed throughout the period of sediment deposition. This does not mean, however, that lake levels must have remained steady relative to the sill depth. Today, during periods of overflow, lake level has risen at least 40 cm above the elevation of the sill (Morrill, 2004). Lake level fluctuations of this size are large enough to cause variations in the amount of *Potamogeton*.

Transition 2 (4700 cal yr B.P.)

The third PC shows a step change that is significantly correlated to a shift in the $\delta^{18}\text{O}$ record to less negative values (Table 4, Fig. 3). We infer that monsoon precipitation decreased and the residence time of water in the lake increased at this time. The shift in $\delta^{18}\text{O}$ values is also apparent in measurements using *Potamogeton* encrustations (Fig. 3), indicating that it reflects changes in the $\delta^{18}\text{O}$ of DIC rather than detrital influence. Unlike Transition 1, *Potamogeton* did not become more abundant at this time. This might be explained by the non-linear response of this proxy to lake depth (Fig. 4).

Late Holocene (<4000 cal yr B.P.)

The cores do not contain sediment from the last ~4000 calendar years. We argue that the lake was too shallow to accumulate sediments during some or all of this time. When lake level falls below a critical depth in very shallow lakes, wind mixing increases, sediment will cease to be deposited and previously deposited sediments can be eroded (Verschuuren, 1999; Douglas and Rippey, 2000). Desiccation of the lake and deflation of exposed sediments are also possible, but we have found no evidence for this, such as unconformities or changes in sediment texture. It is more probable that the lake became shallower but did not completely desiccate. The possibility of sediment erosion makes it impossible to say at what times the lake was too shallow for sediment accumulation. A similar drop in lake level can explain changes between 5000 and 6000 cal yr B.P., when the

sedimentation rate of core 2A decreased and there was a period of erosion and/or non-deposition in cores 3A and 4A. The large increase in $\delta^{18}\text{O}$ values in core 2A at the start of this interval supports this interpretation. Under this scenario, the more complete sediment record of core 2A might be explained by spatial variations in mixing and sediment focusing on the bottom of the lake.

Sediment infilling through the Holocene contributed to low lake levels during the late Holocene, but it cannot be the sole explanation. Infilling alone would lead to a decrease in lake volume, a decrease in lake-water residence time and decreased $\delta^{18}\text{O}$ values. Instead, we find an increase in $\delta^{18}\text{O}$ values through the Holocene (Fig. 6), consistent with declining monsoon precipitation.

We did not recover the top 1 or 2 cm of surface sediments during coring. Bulk organic matter in surface sediments in shallower parts of the lake has ^{14}C activities between ~93 and 99% (Table 1). The $\delta^{13}\text{C}$ values of these samples and visual examination of the sediments indicate that most of the organic matter is lacustrine algae. It is difficult to assign an exact age to these sediments because of large recent variations in atmospheric ^{14}C due to bomb testing. It is clear, however, that these sediments are not ~4000 yr old. Assuming a hard-water correction similar to that measured in modern *Potamogeton*, these samples yield ^{14}C activities between ~100 and 107%, suggesting they contain a mixture of bomb and pre-bomb radiocarbon. Therefore, during the 20th century and possibly earlier, sediment accumulated in the lake, probably due to increased lake level and monsoon precipitation.

Discussion

The sediment record from Ahung Co indicates that monsoon precipitation decreased through the late and middle Holocene following maximum values before 7500 cal yr B.P. Superimposed on this trend are two relatively rapid decreases in monsoon rainfall at 7000–7500 and 4700 cal yr B.P. and several wet–dry oscillations with a median spacing of ~500 yr (range: 200 to 1650 yr). At one or more times after 4000 cal yr B.P., the lake probably became too shallow for sediment deposition and increased wind mixing caused sediment erosion and/or resuspension. Similar conditions might have existed between 5000 and 6000 cal yr B.P. when the sedimentation rate of core 2A decreased and there was a period of erosion and/or non-deposition in cores 3A and 4A. Surface sediments in the lake accumulated during the 20th century and possibly earlier. The age of these recent sediments is not well constrained, but we speculate that they correlate to an increase in monsoon strength during the past 400 yr inferred by Anderson et al. (2002) for the Indian Ocean.

This is the first water-balance record from Tibet to have an age model based on terrestrial material. Our results illustrate a problem in using core-top dates from aquatic plant material to determine the hard-water effect, a method used for other Tibetan lakes. It is nearly impossible to distinguish between a sedimentary gap at the top of the core due to low lake level and

a large hard-water effect. Measurements of ^{14}C activity in the modern lake can indicate the expected hard-water effect. However, changes in the hard-water effect through time must also be considered.

A decrease in monsoon strength through the Holocene is apparent in other records, including those from Sumxi Co, Bangong Co, the Arabian Sea, Oman and elsewhere (Fig. 8; Gasse et al., 1991, 1996; Overpeck et al., 1996; Liu et al., 1998; Fleitmann et al., 2003). This is expected given declining summer insolation through the Holocene. During the summer,

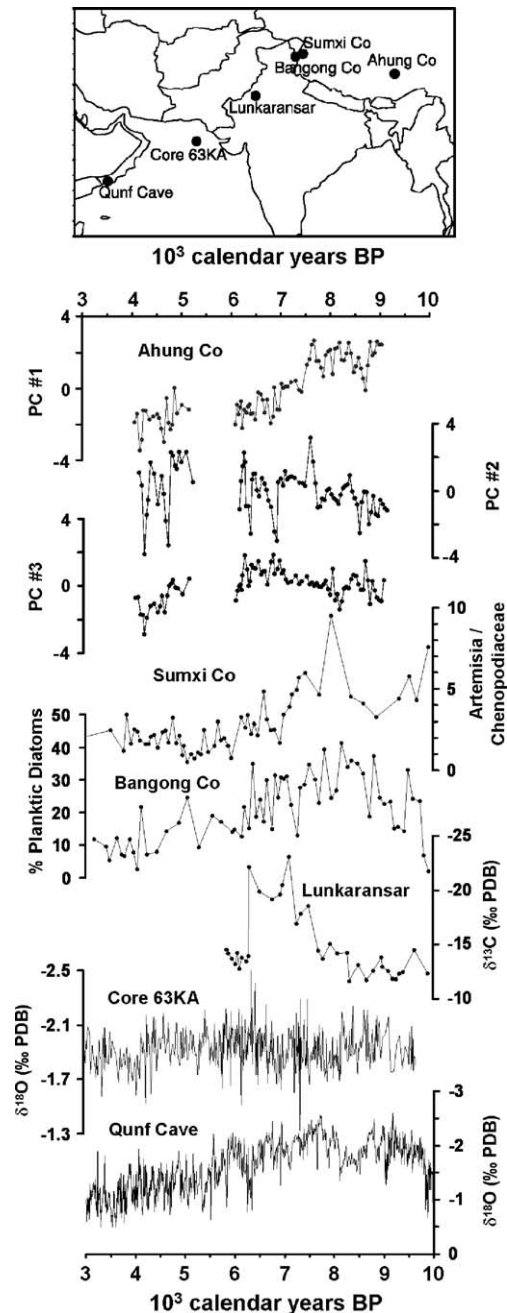


Figure 8. High-resolution records of southwest Asian monsoon. All y axes are oriented such that periods of increased monsoon precipitation plot towards the top of the figure. Data from: Ahung Co, this study; Sumxi Co, Gasse et al. (1991); Bangong Co, Gasse et al. (1996); Lunkaransar, Enzel et al. (1999); Core 63KA, Staubwasser et al. (2002); Qunf Cave, Fleitmann et al. (2003).

temperatures over Asia increase more than temperatures over the Indian Ocean due to the higher specific heat of water. This results in a temperature gradient that fuels the monsoon circulation. When summer insolation is lower, the temperature contrast between land and ocean is less pronounced and the monsoon circulation is weaker.

Rapid decreases in monsoon precipitation, such as those we inferred for 7000–7500 and 4700 cal yr B.P., are less consistent among nearby records (Fig. 8). This could be the result of (1) regional differences in monsoon history, (2) the influence of climatic variables other than monsoon precipitation, (3) local environmental changes such as neotectonics or changes in sill elevation, and/or (4) a non-linear response of proxies to environmental change, causing abrupt shifts in the proxies that do not correspond to an abrupt climate change. We argue for several reasons that the two transitions we documented at Ahung Co reflect changes in monsoon precipitation. First, a synthesis of 36 previously published records from across the Asian monsoon region showed an abrupt weakening in monsoon strength at 4500–5000 cal yr B.P. (Morrill et al., 2003). Second, some records from southwest Asia, including Sumxi Co, Bangong Co, and Qunf Cave show a first decrease in monsoon strength at ~7000 cal yr B.P., following the early Holocene maximum (Fig. 8). Short events like the wet–dry oscillations observed at Ahung Co are difficult to compare between records due to coarse resolution and dating uncertainties. As more high-resolution records are published, we will be able to determine whether this century-scale variability is spatially coherent.

The causes of past monsoon variations are under debate. Possibilities include: changes in solar irradiance, temperature variations in the North Atlantic, and changes in the intensity and frequency of El Niño events (see review in Morrill et al., 2003). For many records, including Ahung Co, it is difficult to make a compelling case for any one of these factors controlling precipitation. Noise and dating uncertainties in both monsoon records and forcing time-series impede comparisons. It is also possible, and perhaps likely given the complexity of the climate system, that there are multiple causes that interact with one another.

Conclusions

- The sediment record from Ahung Co shows two abrupt declines in monsoon precipitation at 7000–7500 and 4700 cal yr B.P. In some records from southwest Asia, the first decrease in monsoon precipitation following the early Holocene monsoon maximum occurs at about 7000 cal yr B.P. The event at 4700 cal yr B.P. corresponds to a widespread, abrupt weakening of the Asian monsoon (Morrill et al., 2003).
- There were several (~7) multi-century fluctuations in Ahung Co between states dominated by aquatic macrophytes and by lacustrine algae. These occurred with a median spacing of 500 yr (range: 200–1650 yr). We argue based on a correspondence between the macrophyte layers

and higher $\delta^{18}\text{O}$ values that these fluctuations were triggered by changes in lake level.

- At times during the last 4000 cal yr, the lake was too shallow for sediment accumulation. The exact duration of the lowstand(s) is unknown due to the possibility of sediment erosion and/or deflation.
- Surface sediments in the lake accumulated during the 20th century. Their age is not well constrained, but we speculate that they correlate to a recent increase in monsoon strength (Anderson et al., 2002).

Acknowledgments

We thank J. Quade, D. Dettman and J. Shuttleworth for helpful discussions and two anonymous reviewers for helpful comments. This work was supported by grants from the NSF Earth System History program, NSF Graduate Fellowship program, NASA Space Grant program and Geological Society of America. We thank S. Trumbore, T. Jull, T. Lange and L. Hewitt for help with radiocarbon dating and S. Elias for insect identification. We thank H. Barnett, C. Urban-Evans, T. Dzienis and W. Wheeler for laboratory assistance.

References

- An, Z., Porter, S.C., Kutzbach, J.E., Wu, X., Wang, S., Liu, X., Li, X., Zhou, W., 2000. Asynchronous Holocene optimum of the East Asian monsoon. *Quaternary Science Reviews* 19, 743–762.
- Anderson, D.M., Overpeck, J.T., Gupta, A.K., 2002. Increase in the Asian southwest monsoon during the last four centuries. *Science* 297, 596–599.
- Araguas-Araguas, L., Froehlich, K., Rozanski, K., 1998. Stable isotope composition of precipitation over southeast Asia. *Journal of Geophysical Research* 103, 28721–28742.
- Baker, F.C., 1945. *The Molluscan Family Planorbidae*. University of Illinois Press, Urbana, Illinois.
- Barnett, T.P., Dumenil, L., Schlese, U., Roeckner, E., 1988. The effect of Eurasian snow cover on global climate. *Science* 239, 504–507.
- Blind, I., Andersson, G., Hargeby, A., Johansson, S., 1993. Long-term pattern of alternative stable states in two shallow eutrophic lakes. *Freshwater Biology* 30, 159–167.
- Chang, C., Shackleton, R.M., Dewey, J.F., Yin, J., 1988. *The Geological Evolution of Tibet: Royal Society-Academia Sinica Geotraverse of the Qinghai-Xizang Plateau 1985*. Royal Society, London.
- Coops, H., Doef, R.W., 1996. Submerged vegetation development in two shallow, eutrophic lakes. *Hydrobiologia* 340, 115–120.
- Deevey Jr., E.S., Gross, M.S., Hutchinson, G.E., Kraybill, H.L., 1954. The natural ^{14}C contents of materials from hard-water lakes. *Proceedings of the National Academy of Sciences* 40, 285–288.
- Douglas, R.W., Rippey, B., 2000. The random redistribution of sediment by wind in a lake. *Limnology and Oceanography* 45, 686–694.
- Engel, S., Nichols, S.A., 1994. Aquatic macrophyte growth in a turbid windswept lake. *Journal of Freshwater Ecology* 9, 97–109.
- Enzel, Y., Ely, L.L., Mishra, S., Ramesh, R., Amit, R., Lazar, B., Rajaguru, S.N., Baker, V.R., Sandler, A., 1999. High-resolution Holocene environmental changes in the Thar Desert, Northwestern India. *Science* 284, 125–128.
- Fleitmann, D., Burns, S.J., Mudelsee, M., Neff, U., Kramers, J., Mangini, A., Matter, A., 2003. Holocene forcing of the Indian monsoon recorded in a stalagmite from Southern Oman. *Science* 300, 1737–1739.
- Fontes, J.-C., Gasse, F., Gibert, E., 1996. Holocene environmental changes in Bangong Co Basin (Western Tibet): Part 1. Chronology and stable isotopes of carbonates of a Holocene lacustrine core. *Palaeogeography, Palaeoclimatology, Palaeoecology* 120, 25–47.
- Gaffey, S.J., Bronnimann, C.E., 1993. Effects of bleaching on organic and mineral phases in biogenic carbonates. *Journal of Sedimentary Petrology* 63, 752–754.
- Gasse, F., Van Campo, E., 1994. Abrupt post-glacial climate events in West Asia and North Africa monsoon domains. *Earth and Planetary Science Letters* 126, 435–456.
- Gasse, F., Arnold, M., Fontes, J.-C., Fort, M., Gibert, E., Huc, A., Li, B., Li, Y., Liu, Q., Melieres, F., Van Campo, E., Wang, F., Zhan, Q., 1991. A 13,000 year climate record from western Tibet. *Nature* 353, 742–745.
- Gasse, F., Fontes, J.-C., Van Campo, E., Wei, K., 1996. Holocene environmental changes in Bangong Co Basin (Western Tibet): Part 4. discussion and conclusions. *Palaeogeography, Palaeoclimatology, Palaeoecology* 120, 79–92.
- Grossman, E.L., Ku, T.L., 1986. Oxygen and carbon isotope fractionation in biogenic aragonite—Temperature effects. *Chemical Geology* 59, 59–74.
- Guo, Z., Petit-Maire, N., Kropelin, S., 2000. Holocene non-orbital climatic events in present-day arid areas of northern Africa and China. *Global and Planetary Change* 26, 97–103.
- Hodell, D.A., Brenner, M., Kanfoush, S.L., Curtis, J.H., Stoner, J.S., Song, X., Wu, Y., Whitmore, T.J., 1999. Paleoclimate of southwestern China for the past 50,000 yr inferred from lake sediment records. *Quaternary Research* 52, 369–380.
- Lister, G.S., Kelts, K., Chen, K., Yu, J., Niessen, F., 1991. Lake Qinghai, China: closed-basin lake levels and the oxygen isotope record for ostracoda since the latest Pleistocene. *Palaeogeography, Palaeoclimatology, Palaeoecology* 84, 141–162.
- Liu, K.-B., Yao, Z., Thompson, L.G., 1998. A pollen record of Holocene climatic changes from the Dunde ice cap, Qinghai-Tibetan Plateau. *Geology* 26, 135–138.
- Liu, Z., Kutzbach, J., Wu, L., 2000. Modeling climate shift of El Niño variability in the Holocene. *Geophysical Research Letters* 27, 2265–2268.
- Lucas, W.J., Tyree, M.T., Petrov, A., 1978. Characterization of photosynthetic ^{14}C assimilation by *Potamogeton lucens* L. *Journal of Experimental Botany* 29, 1409–1421.
- Meyers, P.A., 1994. Preservation of elemental and isotopic source identification of sedimentary organic matter. *Chemical Geology* 114, 289–302.
- Moore, D.M., 1989. *X-ray Diffraction and the Identification and Analysis of Clay Minerals*. Oxford Univ. Press, New York.
- Morinaga, H., Itota, C., Isezaki, H., Goto, H., Yaskawa, M., Kusakabe, J., Liu, Z., Gu, B., Cong, S., 1993. Oxygen-18 and carbon-13 records for the last 14,000 years from lacustrine carbonates of Siling-co lake in the Qinghai-Tibetan Plateau. *Geophysical Research Letters* 20, 2909–2912.
- Morrill, C., 2004. The influence of Asian summer monsoon variability on the water balance of a Tibetan lake. *Journal of Paleolimnology* 32, 273–286.
- Morrill, C., Overpeck, J.T., Cole, J.E., 2003. A synthesis of abrupt changes in the Asian summer monsoon since the last deglaciation. *The Holocene* 13, 465–476.
- Overpeck, J., Anderson, D., Trumbore, S., Prell, W., 1996. The southwest Indian monsoon over the last 18,000 years. *Climate Dynamics* 12, 213–225.
- Overpeck, J., Liu, K., Morrill, C., Cole, J., Shen, C., Anderson, D., Tang, L., 2005. Holocene environmental change in the Himalayan-Tibetan Plateau region: lake sediments and the future. In: Huber, U.M., Bugmann, H.K.M., Reasoner, M.A. (Eds.), *Global Change and Mountain Regions: An Overview of Current Knowledge*. Springer, Boston, pp. 83–92.
- Pewe, T.L., Liu, T., Slatt, R.M., Li, B., 1995. Origin and Character of Loesslike Silt in the Southern Qinghai-Xizang (Tibet) Plateau, China. *United States Geological Survey Professional Paper 1549* (55 pp.).
- Prell, W.L., Kutzbach, J.E., 1992. Sensitivity of the Indian monsoon to forcing parameters and implications for its evolution. *Nature* 360, 647–652.
- Scheffer, M., Hosper, S.H., Meijer, M.-L., Moss, B., Jeppesen, E., 1993. Alternative equilibria in shallow lakes. *Trends in Ecology and Evolution* 8, 275–279.
- Shen, C., 2003. Millennial-scale variations and centennial-scale events in the

- southwest Asian monsoon: pollen evidence from Tibet. PhD Dissertation, Louisiana State University. 286 pp.
- Shukla, J., Paolino, D.A., 1983. The Southern oscillation and long-range forecasting of the summer monsoon rainfall over India. *Monthly Weather Review* 111, 1830–1837.
- Staubwasser, M., Sirocko, F., Grootes, P.M., Erlenkeuser, H., 2002. South Asian monsoon climate change and radiocarbon in the Arabian Sea during early and middle Holocene. *Paleoceanography*, 17.
- Stuiver, M., Reimer, P.J., Bard, E., Beck, J.W., Burr, G.S., Hughen, K.A., Kromer, B., McCormac, G., Van der Plicht, J., Spurk, M., 1998. INTCAL98 radiocarbon age calibration, 24,000–0 cal BP. *Radiocarbon* 35, 215–230.
- Thompson, L.G., Mosley-Thompson, E., Davis, M.E., Bolzan, J.F., Dai, J., Yao, T., Gundestrup, N., Wu, X., Klein, L., Xie, Z., 1989. Holocene–Late Pleistocene climatic ice core records from Qinghai–Tibetan Plateau. *Science* 246, 474–477.
- Thompson, L.G., Yao, T., Davis, M.E., Henderson, K.A., Mosley-Thompson, E., Lin, P.-N., Beer, J., Synal, H.-A., Cole-Dai, J., Bolzan, J.F., 1997. Tropical climate instability: the last glacial cycle from a Qinghai–Tibetan ice core. *Science* 276, 1821–1825.
- Tian, L., Yao, T., Numaguti, A., Sun, W., 2001. Stable isotope variations in monsoon precipitation on the Tibetan Plateau. *Journal of the Meteorological Society of Japan* 79, 959–966.
- Verardo, D.J., Froelich, P.N., McIntyre, A., 1990. Determination of organic carbon and nitrogen in marine sediments using the Carlo Erba NA-1500 Analyzer. *Deep-Sea Research* 37, 157–165.
- Verschuren, D., 1999. Sedimentation controls on the preservation and time resolution of climate-proxy records from shallow fluctuating lakes. *Quaternary Science Reviews* 18, 821–837.
- Wang, B., French, H.M., 1995. Permafrost on the Tibet plateau, China. *Quaternary Science Reviews* 14, 255–274.
- Wang, B., Wu, R., Lau, K.-M., 2001. Interannual variability of the Asian summer monsoon: contrasts between the Indian and the western North Pacific–East Asian monsoons. *Journal of Climate* 14, 4073–4090.
- Wilks, D.S., 1995. *Statistical Methods in the Atmospheric Sciences*. Academic Press, San Diego.
- Winkler, M.G., Wang, P.K., 1993. The late Quaternary vegetation and climate of China. In: Wright, H.E. (Ed.), *Global Climates since the Last Glacial Maximum*. University of Minnesota Press, Minneapolis, pp. 221–261.
- Wright, H.E., Mann, D.H., Glaser, P.H., 1984. Piston corers for peat and lake sediments. *Ecology* 65, 657–659.